JOURNAL OF GEOPHYSICAL RESEARCH, VOL. 100, NO. D6, PAGES 11,509–11,516, JUNE 20, 1995

The role of a deep convective storm over the tropical Pacific Ocean in the redistribution of atmospheric chemical species

Chien Wang,[1] Paul J. Crutzen,[2] and V. Ramanathan
Center for Clouds, Chemistry, and Climate, Scripps Institution of Oceanography, La Jolla, California

Steven F. Williams
Office of Field Project Support, University Corporation for Atmospheric Research, Boulder, Colorado

Abstract. A deep convective storm observed during the Central Equatorial Pacific Experiment (CEPEX) has been simulated using the two-dimensional version of a three-dimensional cloud dynamics, microphysics, and chemistry model. The simulated storm is characterized by the penetration of the cloud tower into the lower stratosphere and by a widespread cloud anvil. Clear evidence of vertical transport of water vapor through the convective turret to the upper troposphere has been found. A large amount of small ice crystals formed in the cloud top and in the anvil together with graupels induced by frozen raindrops. Intense mixing of boundary layer air into the cloud caused by the deep convection can result in low ozone area inside the cloud turret and inside the anvil. However, simultaneously, stratospheric air with high ozone volume mixing ratio was brought into the cloud region in the troposphere, especially in the upper part of the anvil, which could play a significant role in the tropical tropospheric O_3 budget. Due to the deep convection, a significant fraction of boundary layer dimethyl sulfide (DMS) or other ocean-derived chemicals is also transferred to the free troposphere, but we find no evidence for significant transport to the stratosphere.

1. Introduction

Deep convection appears over the western Pacific Ocean more frequently and intensely than in any other region on this planet. Due to the strong vertical transport of water vapor, heat, and momentum and the radiation effect of anvil clouds or cirrus clouds, deep convection in this area is among the most important drivers of atmospheric general circulation. *Ramanathan and Collins* [1991] suggested that the warm sea surface temperature (SST) over the western Pacific Ocean triggers strong and deep convection and that this type of convection would in turn regulate SST itself through the greenhouse effect of increased water vapor and cloud anvil. The Central Equatorial Pacific Experiment (CEPEX) was motivated by Ramanathan and Collins' "thermostat" hypothesis. The primary objective of CEPEX was to evaluate the thermostat hypothesis and to clarify relationships among several key parameters and processes related to it. As well as these crucial issues dealing with atmospheric dynamics and thermodynamics, the interaction between atmospheric chemistry and climate has also been a matter of great interest in this experiment. To interpret the observational data, cloud-scale and large-scale models are used as research tools.

In recent years cloud-scale or cloud ensemble models have been used in studying tropical deep convective clouds. For example, using a two-dimensional cloud model, *Nicholls* [1987] simulated a tropical squall line and compared modeled results with observations. *Krueger* [1988] and *Xu and Krueger* [1991] used a cloud ensemble model to evaluate a parameterization scheme of cloudness for use in large-scale general circulation models (GCMs). *Tao et al.* [1993] compared the heat, moisture, and water budget of midlatitude squall lines with those over tropical regions. *Wong et al.* [1993] studied the impact of mesoscale convective systems on the radiative budget of atmosphere. The majority efforts in simulating tropical convection traditionally focused on important radiative effects or energy budgets. However, as suggested by *Chatfield and Crutzen* [1984], rapid vertical transport by convective clouds are also important to atmospheric chemistry, especially if it affects the formation of sulfate aerosols or ozone. Recent observations show the evidence of direct transport of tropospheric air into the low tropical stratosphere induced by deep convections [*Danielsen*, 1993; *Kritz et al.*, 1993]. This process, accompanied by transport of certain chemical species, will impact on the stratospheric chemistry [*Solomon et al.*, 1994].

This paper summarizes our preliminary modeling efforts in simulating the redistribution of chemical species by the deep convective clouds over the tropical Pacific Ocean. Observational data from CEPEX have been used to initialize our model. We first briefly describe the model and the data used in the simulation. Next we show and discuss the model results regarding the cloud structure and evolution including the water vapor redistribution. Thereafter, we discuss the redistributions of important chemical

[1]Now at Massachusetts Institute of Technology, Cambridge.
[2]Also at Max-Planck-Institut für Chemie, Mainz, Germany.

Paper number 95JD01173.
0148-0227/95/95JD-01173$05.00

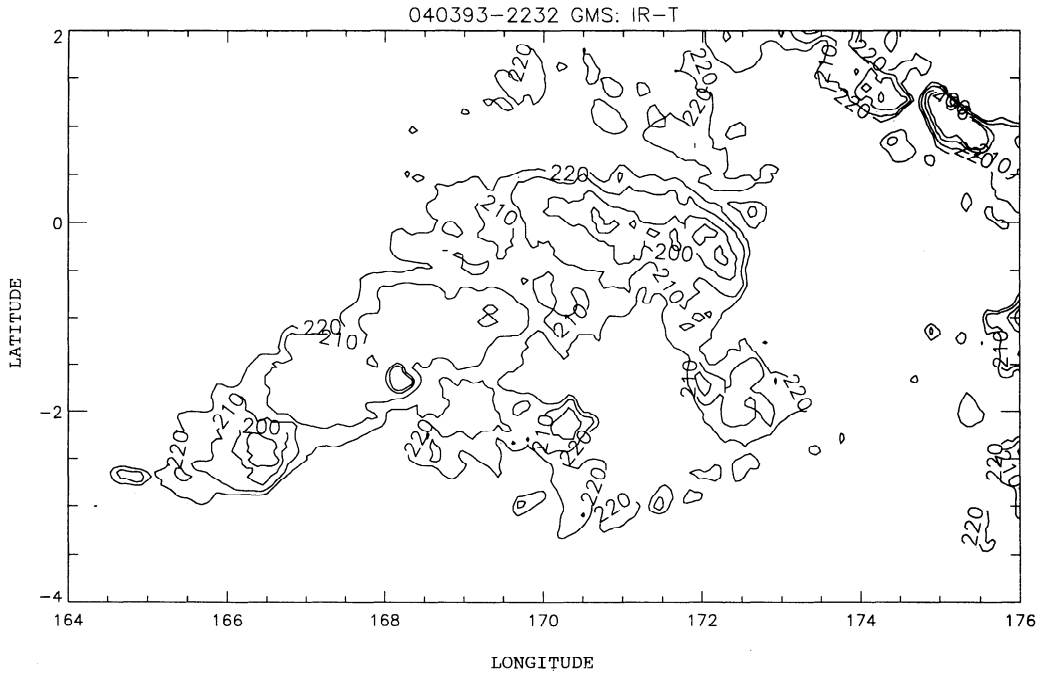

Figure 1. Horizontal distribution of GMS brightness temperature at 2232 (UTC) on April 3, 1993. Contour lines represent infrared temperature from 200 to 220 K with 10-K intervals. The horizontal axis represents longitude and the vertical axis represents latitude (in degrees).

species, in particular ozone and dimethyl sulfide (or DMS, which is CH_3SCH_3).

2. Description of Model

Two models have been used in this study. The first one is the two-dimensional version of a three-dimensional model of cloud dynamics and microphysics [*Wang and Chang*, 1993]. This model is an elastic and nonhydrostatic one. It can simulate the evolutions of wind speeds, air temperature, air pressure or density, the mixing ratio of water vapor, and the mixing ratios and number concentrations of six condensed water categories (cloud drop, raindrop, ice crystal, snowflake, graupel, and hailstone). A so-called semispectra microphysical scheme adopted in the model uses two parameters, that is, both mixing ratio and number concentration of each water category, to calculate microphysical transformations based on the size spectrum of cloud droplets. To save computational time and reduce data storage space, we used a simplified version derived from the original model. In this version, only two ice phase categories have been included, compared with four categories in the original model. The ice crystal category in the simplified version combines the ice crystal and snowflake groups of the original model, while graupel represents the combination of graupel and hailstone. Therefore, ice crystals can be interpreted as unrimed ice particles and graupels as frozen raindrops or rimed ice particles. Under the environmental conditions we used in this modeling study, the possible difference of these two model versions caused by the different behavior between ice crystals and snowflakes or graupel and hailstones is rather less important for the primary goal of this study, that is, modeling of the dynamical and thermodynamical features of the storm. Differences of terminal falling speeds between the two pairs are quite small compared to the vertical velocity of air motion in the simulated storm.

The second model is a cloud transport model, which is driven by the meteorological field provided by the cloud dynamics and microphysics model and calculates the mixing ratios of chemical species. It does not include interactions with the aqueous phase so chemical species are treated as passive tracers, restricting the applicability of the model to gases of low solubility and long residence times relative to the temporal evolution of the convection. As most gases that are emitted at the Earth's surface belong to this class, this is no severe restriction. In this paper we will apply it to the cloud transport of DMS and ozone. The continuity equation for chemical species in this model takes the following form:

$$\frac{\partial C}{\partial t} + \frac{\partial C U_j}{\partial x_j} - C\frac{\partial U_j}{\partial x_j} = E_c \qquad (1)$$

where C represents the gaseous phase concentration of any given chemical species, t represents time, U is the wind speed, E_c is the subgrid scale term, and x_j represents the coordinate axis. The concentrations of chemical species are defined in a staggered coordinate system in conjunction with horizontal and vertical wind speeds. One important issue in numerical simulation of atmospheric chemistry is the advection problem. In the cloud transport model the same positive-definite advection scheme as used in the cloud chemistry model [*Wang and Chang*, 1993] has been adopted.

In this study we set the horizontal grid spacing at 1 km and that in the vertical grid at 500 m. With 500 horizontal and 50 vertical grid points the model domain covers 500 km horizontally and 25 km vertically. The output data of the cloud physics model are archived for every 3 min. The data, including wind speed, air temperature, pressure, density,

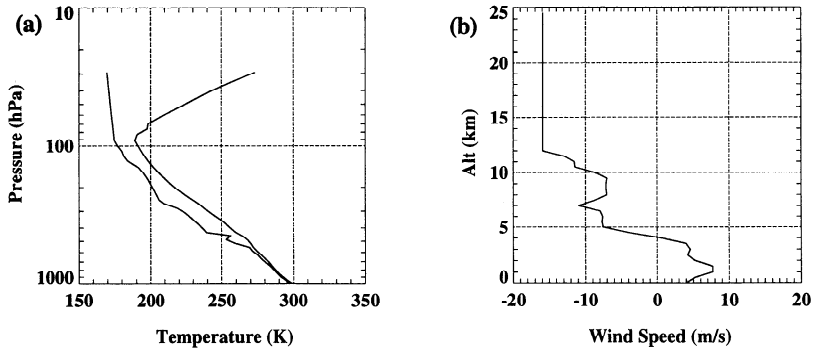

Figure 2. Initial profiles used in simulation of (a) temperature and dew point temperature as functions of air pressure and (b) horizontal wind speed as a function of altitude.

mixing ratio of water vapor, etc., are used to drive the cloud transport model to calculate the gaseous phase concentrations of chemical species.

3. CEPEX April 3 Case and Cloud Simulation Results

The case chosen in this study is the April 3 case during CEPEX, consisting of an intense cluster with several convective towers. The satellite infrared image (Figure 1) showed that this system was located between 165°E and 173°E and 3°S and 1°N at 2232 (UTC) April 3, 1993. The size of the anvil formed by the north tower was about 500 km in the west-east direction and 150 km in the north-south direction. In this area the brightness temperature below 200 K (at least 15 km in cloud top height) has been observed. The satellite observations also showed that the lifetime of the whole system was about 2 days; those for the individual towers were shorter than this.

Between 2220 and 2358 UTC, four dropsondes were released from a Learjet aircraft along the 2°S between 177.44°E and 170°E. Because the one released at 2324 UTC positioned at 172.04°E and 2.02°S was the closest to the north tower, it was chosen as the initial profile for this study (Figure 2). As the dropsonde observation only provided profiles from 7 km to the surface, we used the regular sounding from the island of Funafuti (179.22°E, 8.52°S) to cover the layers above 7 km. The initial field of the model was assumed to be horizontally homogeneous. To initiate the convection, a warm bubble 10 km wide and 2.5 km high with a maximum temperature deviation of 1.45 K was triggered in the boundary layer at the start of the simulation. There was no initial large-scale lift imposed. The simulation lasted for about 3 hours until the west edge of cloud anvil approached the lateral boundary of the model.

After 165 min the simulated deep convective storm developed a deep penetrative tower and a widespread anvil which propagated to the west (Figure 3). Its top reached close to 20 km height. The most active part of the cloud was only about 40 km wide in the lower troposphere. However, the high water-loading region, where the total condensed water content is higher than 4 g kg^{-1}, occupied a 100-km-wide area in the upper troposphere just below the tropopause. This shows that the storm we simulated had grown to its mature stage. In the lower anvil, or stratiform part of the cloud, weak precipitation has already formed. Some rainwater from this part of the cloud actually was reaching the surface. Initial airflow pattern in the boundary layer has been changed because of the development of the storm. It appeared as flowing into the cloud tower from both the east and west sides of the cloud body in the mature stage. In the higher level of free troposphere the direction of airflow was primarily controlled by the initial wind. However, cloud outflows significantly influenced the wind field by changing the horizontal wind speeds in these areas.

We found that in the mature stage of the storm, as expected, ice phase particles are the dominant component of the cloud water hydrometeors above 10 km and account for more than 90% in total water content including water vapor (Figure 4). In a small area near the cloud top, the ratio of the ice phase water to total water content was even close to 100%. Liquid water accounts for about 20% of the total water mass including water vapor in those parts of convec-

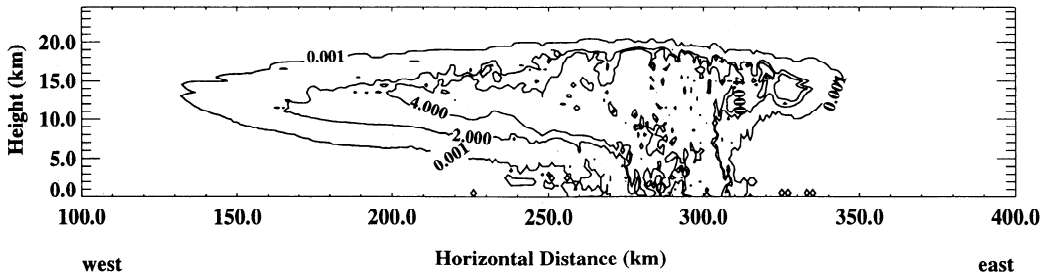

Figure 3. Mixing ratio of total condensed water including cloud water, rainwater, ice crystal, and graupel at 165 min of simulation time. Contour lines represent mixing ratios of 0.001, 2.001, and 4.001 g kg^{-1} with intervals of 2 g kg^{-1}.

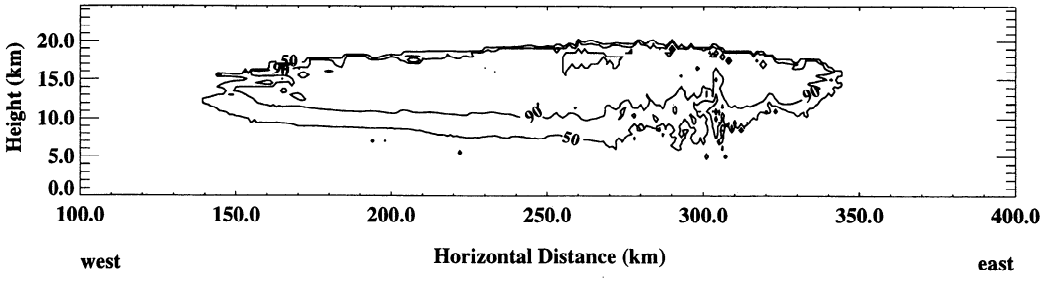

Figure 4. Percentage of ice water content in total water content including total condensed water and water vapor at 165 min of simulation time. Contour lines represent values of 50%, 90%, and 100%.

tion tower below 10 km. From the simulated results we also found that the number concentrations of ice phase particles in the upper cloud layer and anvil were very high, several hundred per liter, which is very close to the aircraft observational results (G. M. McFarquhar and A. J. Heymsfield, In-situ observations of the horizontal and vertical structure of three cirrus anvils sampled during the Central Equatorial Pacific Experiment (CEPEX), submitted to *Journal of the Atmospheric Sciences*, 1995, hereinafter referred to as submission, 1995). The size-spectral-mean diameter of ice crystals is about 30 to 40 μm in most parts of the cloud, that of graupel is at least 1 order of magnitude larger. Considering the number concentration of ice crystals, we infer that it is possible that a large amount of small ice crystals existed inside this storm.

The intense convection induced by the simulated storm caused a significant redistribution of water vapor. From Figure 5 we can see that inside the convective tower, the mixing ratio of water vapor in the mature stage is somewhere around the initial value of the layer at least 3 km lower (the initial field of water vapor was horizontally homogeneous). In a layer near the cloud top, corresponding to the initial tropopause (about 17 km high) and located between 250 and 300 km from the west boundary of the model domain, we find that the mixing ratio of water vapor is lower than that of the surrounding air. The dehydration in this area was induced by the diffusive growth of ice crystals, which tend to form very low mixing ratios due to the existence of the lowest tropospheric temperature in this region. However, above 19 km and up to 21 km water vapor mixing ratios increase again in a thin layer. It is the result of evaporation of the ice crystals in this part of lower stratosphere. This feature was also observed in the balloon observation [*Vömel et al.*, 1993]. They measured the lowest water vapor mixing ratio around the tropopause at 16.7 km in the CEPEX regions with deep convections. They also found that the water vapor mixing ratio increased sharply above the tropopause, peaking at 20 km in the warm pool region.

4. Redistribution of Ozone and DMS

We used the O_3 sounding released on March 9, 1993, from the R/V *Vickers* to initiate our O_3 simulation. The surface volume mixing ratio of O_3 from this sounding is 7 parts per billion by volume (ppbv). To investigate the impact of deep convection, we have smoothed the original profile between 8 km and 15 km height, which appeared to be fluctuating around 10.5 ppbv, by applying a constant volume mixing ratio of 10.5 ppbv. We also assumed that DMS only existed inside the boundary layer initially with a volume mixing ratio of 40 parts per trillion by volume (pptv) [*Thornton and Bandy*, 1993]. The initial profiles for concentrations of O_3 and DMS are plotted in Figure 6.

4.1. Ozone Simulation

The O_3 redistribution caused by transport and mixing in the mature stage of the simulated storm is significant (Figure 7). In the absence of photochemical enhancement, air masses with low ozone concentrations from the boundary layer were mixed into the free troposphere. Inside the convective tower and in the middle part of the anvil (~12.5 km height), volume mixing ratios of O_3 were reduced to about 9 ppbv, which is equal to the initial value of ozone below 1.5–2 km height. At the same time a considerable amount of air with high O_3 volume mixing ratio was brought into the cloud region, especially in the upper part of the anvil. From Figure 7 we find that the 11 ppbv contour line (initially above 16 km) had already extended to below 15 km height and spread horizontally along the anvil. In the vicinity of the strongest updraft region (between 250 and 280 km from the west boundary of model domain), substantial exchange between air from the troposphere and the strato-

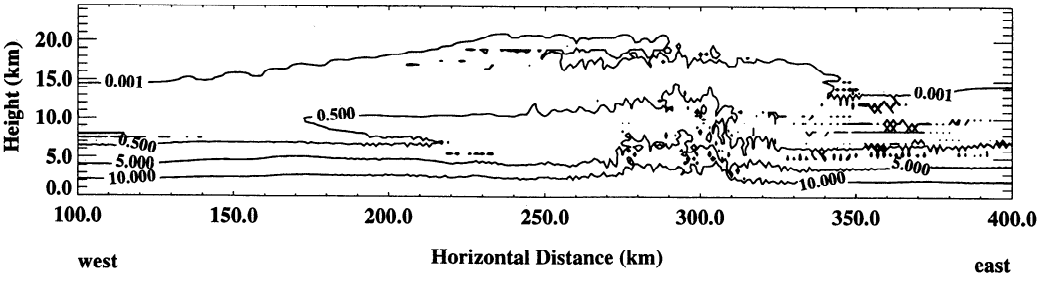

Figure 5. Distribution of modeled mixing ratio of water vapor after 165 min of simulation time. Contour lines represent values of 0.001, 5.0, and 10.0 g kg^{-1}.

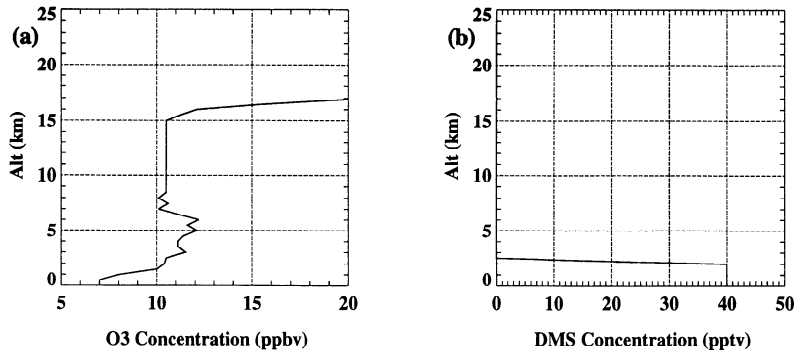

Figure 6. Initial profiles in simulation of (a) volume mixing ratio of ozone in ppbv and (b) DMS in pptv as functions of altitude.

sphere took place. The deepest intrusion of high O_3 air (O_3 mixing ratio $\geq$40 ppbv) reached down to 12.5 km height in a location around 250 km from the west boundary of the model domain.

The air exchange described above can be shown even more clearly from the horizontal distribution of O_3 volume mixing ratio at selected heights in the mature stage of the simulated storm (Figure 8). The ozone mixing ratio profile at 17 km (Figure 8b) clearly reveals penetration of tropospheric air to the lower stratosphere. For example, between 260 km and 380 km from the western boundary the mixing ratios dip to 10 ppbv, equal to the initial values at 15 km. Between 180 km and 260 km in horizontal distance, O_3 volume mixing ratios are much higher than the initial value, indicating substantial intrusion of stratospheric air. The same feature with volume mixing ratios approaching 60 ppbv can still be observed at the 15-km level (Figure 8a) near 250 km, where 10.5 ppbv was the initial mixing ratio of O_3. All regions with ozone volume mixing ratios higher than 10.5 ppbv contain a fraction of stratospheric air. Although the penetration of cloud air into the stratosphere would cause lower ozone mixing ratios, the tiny decrease induced by the updraft is easily compensated by downward mixing of air with much higher O_3 concentration. From Figure 8c we can see that the decreases of ozone volume mixing ratios at 19 km level were primarily induced by the upward transport of air parcel from a layer between 17 and 19 km height. The impact of direct transport of tropospheric air to the lower stratosphere on the ozone mixing ratio is very limited. From these result we conclude that, although deep convection can lift O_3-poor air from the boundary layer to the upper troposphere and even to the lower stratosphere, the convection also can induce a downward intrusion of air rich in ozone into the cloud and its environs. Our results thus suggest the possibility not only of significant upward transport of tropospheric air into the stratosphere in the tropics, as indicated by *Danielsen* [1993] and *Kritz et al.* [1993], but also of stratospheric ozone into the troposphere. This process can play a particularly significant role in the CEPEX domain containing otherwise such low ozone concentrations.

4.2. DMS Simulation

The model simulation also suggests that significant amounts of gaseous DMS can be transported upward from the marine boundary layer to the upper troposphere and to a small degree even into the lower stratosphere by the deep convection. In the mature stage of the storm inside the cloud tower, volume mixing ratio of DMS reached about 10 pptv (Figure 9). In addition, within the middle and lower part of the cloud anvil, concentration of DMS can be higher than 1 pptv. The horizontal distance of this high-DMS area is about 100 km with an upward extension to about 19 km.

To investigate the relative transport efficiency of DMS, a diagnostic parameter has been derived based on our simulation results:

$$R = \mathrm{DMS}(t, x, z)/\mathrm{DMS}(0) \quad (2)$$

where DMS(0) represents the initial volume mixing ratio inside boundary layer, DMS(t, x, z) represents DMS mixing ratio at a given time step and given spatial position. Figure 10 shows the distribution of R (in percent) at 165 min of simulation time. Within the convective tower, R is generally higher than 25%. In the eastern part of the tower, R is higher than 50% in a column ranging from the surface to about 11 km height. The top of the 25% contour line reached about 15

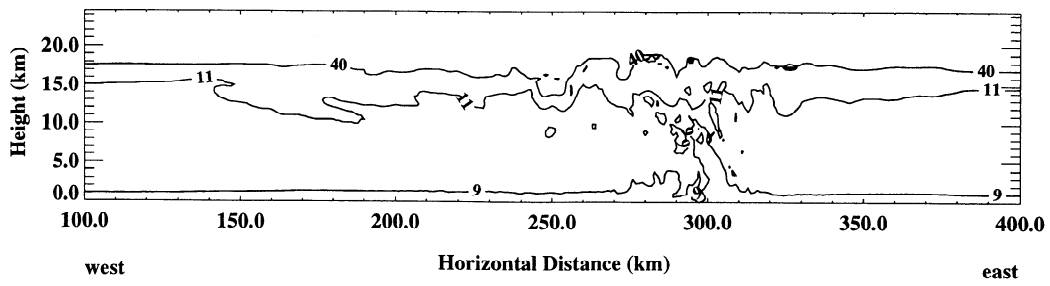

Figure 7. Distribution of ozone mixing ratio after 165 min of simulation time. Contour lines represent ozone mixing ratio values of 9, 11, and 40 ppbv.

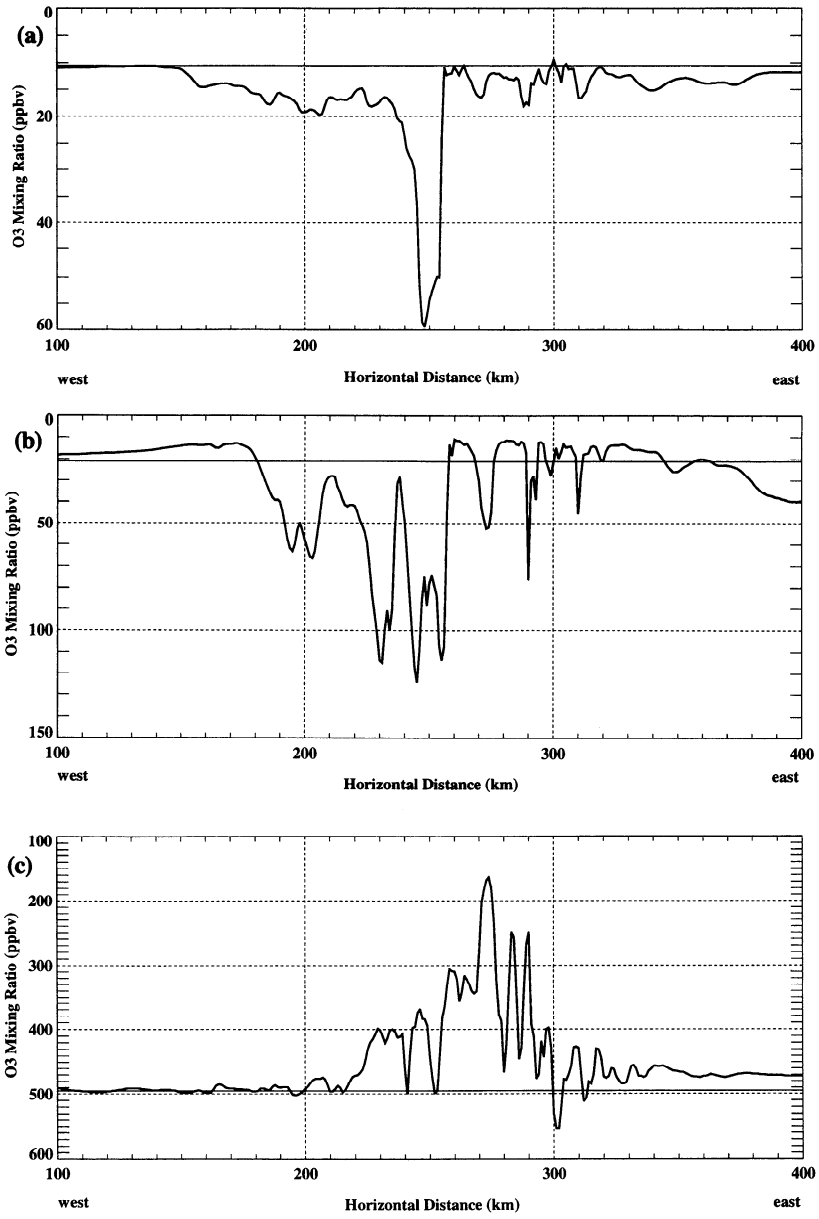

Figure 8. Simulated horizontal distribution of volume mixing ratio of ozone in ppbv at (a) 15 km, (b) 17 km, and (c) 19 km height after 165 min of simulation time. The thin solid line represents initial value of ozone mixing ratio at the given height. The dark line shows the calculated ozone mixing ratios at 165 min.

km height. This implies that inside the convective tower and up to about 15 km, more than 25% of the air had come from the boundary layer, or, in other words, the mixing ratio of DMS in this area can reach at least 1/4 of that inside the marine boundary layer. However, we also found that in the upper part of the cloud tower (above 15 km) and in most of the anvil, the relative transport efficiencies of DMS are rather low, signifying strong dilution with free tropospheric

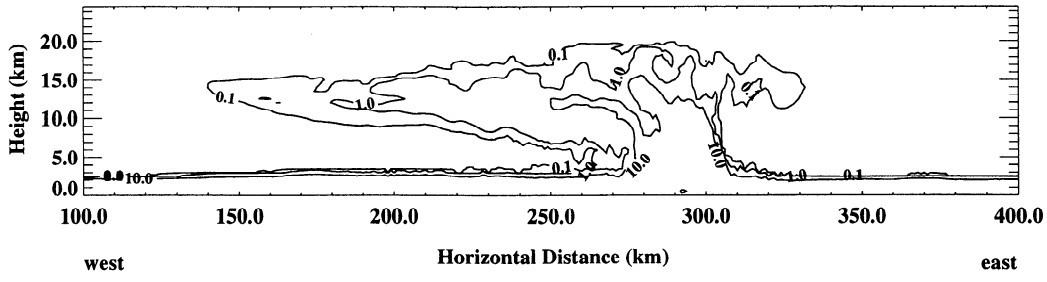

Figure 9. Simulated distribution of DMS mixing ratio in pptv after 165 min. Contour lines represent values of 0.1, 1.0, and 10.0 ppbv.

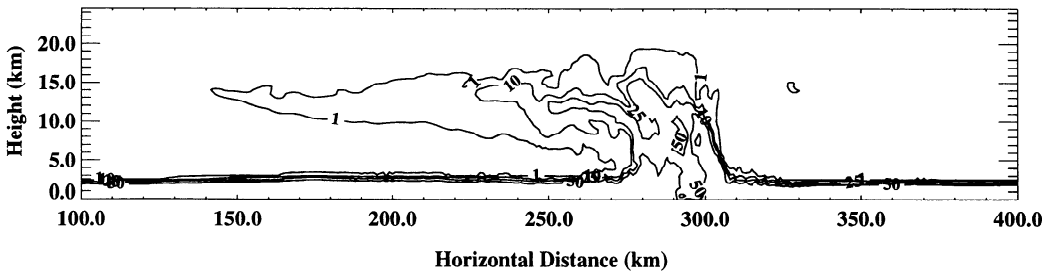

Figure 10. Distribution of R, the ratio of DMS mixing ratio after 165 min to initial DMS mixing ratio inside the marine boundary layer. Contour lines represent values of 1%, 10%, 25%, and 50%.

air. The typical values of R in these regions are between 1% and 10%, which means the mixing ratio of DMS can only reach a level lower than 10% of that in the boundary layer.

Nevertheless, it is clear that a significant fraction of boundary layer DMS can be transported to the upper troposphere and a small fraction even into the lower stratosphere, where oxidation processes initiated by reaction with OH can lead to the formation of sulfur dioxide, methane sulfonic, and sulfuric acid, and ultimately to aerosol particles that may serve as cloud condensation nuclei (CCN), processes that are favored by the low temperatures in the upper troposphere. Compared to the model of *Chatfield and Crutzen* [1984], it appears, however, that the contribution of DMS to the upper troposphere may be quite small. Although our model allowed for some transport of DMS into the stratosphere, the calculated volume mixing ratios in the top of convective tower is in the order of 10^{-1} pptv, compared to the 40 pptv in the marine boundary layer that was assumed here. Our model results would thus indicate that transfer of S from the troposphere to the stratosphere by reactive DMS is small compared with that supplied by carbonyl sulfide (COS) that is present in the troposphere with a rather uniform volume mixing ratio of 600 pptv. Similar conclusion regarding rather inefficient transfer of reactive boundary layer gases to the lower stratosphere by convective activity also may apply to other gases, such as CH_3I, which has been invoked by *Solomon et al.* [1994] to play a role in the ozone photochemistry in the lower stratosphere. However, we propose nevertheless that in light of the great potential importance of this issue, measurements are being made to verify our theoretical findings.

5. Discussion and Summary

The development of a tropical deep convective storm observed during CEPEX has been simulated using two-dimensional cloud-scale models. Observational data including dropsondes, island soundings, and O_3 sounding from shipboard have been used to initiate the model. Simulated results include cloud microphysical, dynamical, and thermodynamical structure and evolution and their effects on the redistributions of ozone and DMS.

The simulated storm was characterized by a deep-penetrating tower and a widespread anvil. Our results suggest the existence of small ice crystals (mean diameter of ice crystals about 30 to 40 μm) with concentrations as high as 10^2 per liter of air in the cloud tower or anvil, which is close to the observations (G. M. McFarquhar and A. J. Heymsfield, submission, 1995). Ice phase water content accounts for more than 50% of the total water content including water vapor in most areas of the cloud. Above about 10 km height the ice phase water can contain even more than 90% in the total water content. Clear evidence of vertical transport of water vapor through the convective turret to the upper troposphere has been found. The model also predicted the existence of a thin layer with comparably higher water vapor mixing ratio in the lower stratosphere (19–21 km height, about 2–4 km above the initial tropopause height) induced by the evaporation of ice crystals. This layer was located just above a dehydration layer [e.g., *Danielsen*, 1993; *Kelly et al.*, 1993] around the initial tropopause at 17 km height formed by diffusive growth of ice crystals. This pattern repeats the same phenomenon observed during CEPEX and indicated by *Vömel et al.* [1993].

The intense mixing and transport induced by the storm causes a decrease of ozone volume mixing ratios inside the cloud tower, especially in the middle and lower part, and in some areas in the middle of anvil. The deep convection also causes intrusion of stratospheric air with higher O_3 volume mixing ratio into the upper troposphere down to 12.5 km. Around the level of tropopause, intense air exchange has been found. Corresponding to the cloud tower, considerable upward transport of air parcels takes place, while in other region corresponding to the anvil part of the cloud, air parcels with much higher ozone concentration than the original air are found.

We found that based on our simulation, the simulated deep convective storm can transport a significant amount of DMS from marine boundary layer into the free troposphere. Inside a considerable region in the middle and upper troposphere, DMS volume mixing ratios reached about 1/4 of the initial surface mixing ratio values in the mature stage of the storm. The transport efficiency of DMS to the top of the cloud and lower stratosphere, however, turned out to be rather low. The DMS tracer calculations also indicate that a large fraction (>90%) of the air contained in the anvil clouds originated from above the marine boundary layer.

Acknowledgments. This is report 133 of the Center of Clouds, Chemistry, and Climate (C^4), a Science and Technology Center of the National Science Foundation (NSF). This research was funded through the Center of Clouds, Chemistry, and Climate by NSF. Research of the author C. W. in the Massachusetts Institute of Technology is supported by the MIT Joint Program on Science and Policy of Global Change. The authors thank D. Kley, H. G. J. Smit, H. W. Vömel, and S. J. Oltmans for processing and providing ozone sounding data and thank Steve Sherwood for processing dropsonde data. Computational and graphical assistance offered by Erwin Boer and John del Corral is appreciated. Suggestions from two anony-

mous reviewers and discussions with Greg McFarquhar and Mary Barth were very helpful.

References

Chatfield, R. B., and P. J. Crutzen, Sulfur dioxide in remote oceanic air: Cloud transport of reactive precursors, *J. Geophys. Res.*, *89*(D5), 7111–7132, 1984.

Danielsen, E. F., In situ evidence of rapid, vertical, irreversible transport of lower tropospheric air into the lower tropical stratosphere by convective cloud turrets and by larger-scale upwelling in tropical cyclones, *J. Geophys. Res.*, *98*(D5), 8665–8681, 1993.

Kelly, K. K., M. H. Proffitt, K. R. Chan, M. Loewenstein, J. R. Podolske, S. E. Strahan, J. C. Wilson, and D. Kley, Water vapor and cloud water measurements over Darwin during the STEP 1987 tropical mission, *J. Geophys. Res.*, *98*(D5), 8713–8723, 1993.

Kritz, M. A., S. W. Rosner, K. K. Kelly, M. Loewenstein, and K. R. Chan, Radon measurements in the lower tropical stratosphere: Evidence for rapid vertical transport and dehydration of tropospheric air, *J. Geophys. Res.*, *97*(D5), 8725–8736, 1993.

Krueger, S. K., Numerical simulation of tropical cumulus clouds and their interaction with the subcloud layer, *J. Atmos. Sci.*, *45*(16), 2221–2250, 1988.

Nicholls, M. E., A comparison of the results of a two-dimensional numerical simulation of a tropical squall line with observation, *Mon. Weather Rev.*, *115*, 3055–3077, 1987.

Ramanathan, V., and W. Collins, Thermodynamic regulation of ocean warming by cirrus clouds deduced from observations of the 1987 El-Niño, *Nature*, *351*, 27–32, 1991.

Solomon, S., R. R. Garcia, and A. R. Ravishankara, On the role of iodine in ozone depletion, *J. Geophys. Res.*, *99*(D10), 20,491–20,499, 1994.

Tao, W.-K., J. Simpson, C.-H. Sui, B. Ferrier, S. Lang, J. Scala, M.-D. Chou, K. Pickering, Heating, moisture, and water budgets of tropical and midlatitude squall lines: Comparisons and sensitivity to longwave radiation, *J. Atmos. Sci.*, *50*(5), 673–690, 1993.

Thornton, D. C., and A. R. Bandy, Sulfur dioxide and dimethyl sulfide in the central Pacific troposphere, *J. Atmos. Chem.*, *17*, 1–13, 1993.

Vömel, H. W., S. J. Oltmans, D. Kley, P. J. Crutzen, and H. Nguyen, Balloon-borne observations of stratospheric and upper tropospheric water vapor in the tropics, during CEPEX, *Eos Trans. AGU*, *74*(43), 116, 1993.

Wang, C., and J. S. Chang, A three-dimensional numerical model of cloud dynamics, microphysics, and chemistry, 1, Concepts and formulation, *J. Geophys. Res.*, *98*(D8), 14,827–14,844, 1993.

Wong, T., G. L. Stephens, P. W. Stackhouse Jr., and F. P. J. Valero, The radiative budgets of a tropical mesoscale convective system during the EMEX-STEP-AMEX experiment, 2, Model results, *J. Geophys. Res.*, *98*(D5), 8695–8711, 1993.

Xu, K.-M., and S. K. Krueger, Evaluation of cloudness parameterizations using a cumulus ensemble model, *Mon. Weather Rev.*, *119*, 342–367, 1991.

P. J. Crutzen and V. Ramanathan, Center for Clouds, Chemistry, and Climate, Scripps Institution of Oceanography, La Jolla, CA 92093-0239.

C. Wang, Joint Program on Science and Policy of Global Change, Massachusetts Institute of Technology, Rm. E40-269, Cambridge, MA 02139.

S. F. Williams, Office of Field Project Support, University Corporation for Atmospheric Research, P.O. Box 3000, Boulder, CO 80307.

(Received October 25, 1994; revised March 13, 1995; accepted March 13, 1995.)